JOURNAL OF MATERIALS SCIENCE 20 (1985) 1556–1570

The plastic deformation of ultra-high molecular weight polyethylene

P. F. VAN HUTTEN, C. E. KONING, A. J. PENNINGS
Department of Polymer Chemistry, State University of Groningen, Nijenborgh 16, 9747 AG Groningen, The Netherlands

Gel-spun filaments of different initial morphologies have been subjected to controlled drawing at elevated temperatures. The drawn samples have been examined by high-resolution scanning electron microscopy. The deformation mechanism at temperatures up to 120° C is very similar to crazing, especially in the case of unoriented gel-spun filaments. Filaments exhibiting a shish-kebab morphology offer the opportunity of examining the deformation of elementary fibrils in a quantitative way. The transformation of individual lamellae into fibrils is the initial deformation mode, which is followed by slip of fibrils at a later stage. This is concluded from a comparison of experimental data and model calculations of the maximum draw ratio. Drawing at 144° C results in the formation of globular aggregates of lamellae, with a characteristic long period of 40 nm. This long period persists until all the globules have been converted, by micronecking, into aggregate fibrils of extended-chain character. On a molecular scale, the various processes can be described as the temperature-dependent flow behaviour of an entanglement network.

1. Introduction

The plastic deformation of semi-crystalline polymers has received the attention of many investigators, e.g. Peterlin [1–3], Petermann *et al.* [4], Tarin and Thomas [5], Juska and Harrison [6]. In his "microfibrillar" model, Peterlin [2, 3] describes the transformation of an unoriented structure into a highly anisotropic one. The initial structure is supposed to be spherulitic in nature and to contain a large number of lamellar stacks. As a consequence of its "mosaic" structure, each lamella in the stack is drawn out into several microfibrils during plastic deformation. A stack as a whole, which is composed of a finite number of lamellae, is transformed into a large number of such microfibrils collected in a bundle, which is called a fibril. The plastic deformation which takes place after the transformation of stacks into fibrils has been completed, proceeds mainly by a sliding displacement of fibrils. On a molecular level, the presence of many tie-molecules in the disordered zones within and between microfibrils is envisaged. These tie-molecules are responsible for stress transfer and for the tensile properties of the fibre material.

Juska and Harrison, in their paper [6], suggest that the formation of microfibrils is preceded by local melting of the lamellar material under the influence of tensile stress. In this way, large draw ratios and the existence of an extended-chain crystal nucleus in the microfibrils can be more easily accounted for.

The main problem with regard to any of these deformation models concerns the possibilities of experimental confirmation. It is the purpose of the present paper to provide experimental evidence that will contribute to an understanding of the deformation process. The unique, porous morphology of shish-kebab fibres has furnished the opportunity for a direct visualization of the deformation process. Shish-kebab fibrils have been produced by the techniques of gel-spinning and of stirring-induced crystallization, and the most pertinent morphological aspects of their deformation have been presented in two recent papers [7, 8]. Drawing at moderate temperatures (110 to

0022–2461/85 $03.00 + .12

120° C) has been found to give rise to a transformation process in which the lamellar "overgrowth" on the shish-kebab fibrils is converted into fibrillar segments. In the present work, this transformation will be described more quantitatively by means of a simple model. In addition, the deformation of gel-spun filaments with a more isotropic initial morphology has been studied and will be shown to be very similar to crazing.

Differences in the morphology of gel-spun filaments result from variations in the spinning conditions, in particular the extrusion rate and the extrusion draw ratio [9]. In general, the morphology of a filament is believed to be indicative of the topology of the underlying molecular entanglement network, since a quench solidification of the fluid state, which is in the regime of "cluster flow" [9], takes place after spinning.

In this paper, we will furthermore present electron microscopic observations on the deformation of filaments at 144° C. In combination with small-angle X-ray studies (SAXS) data, these results allow important conclusions concerning the reorganization in the molecular entanglement network during the process of hot-drawing, which is an essential step in the preparation of ultra-strong polyethylene fibres [10, 11].

2. Experimental techniques

2.1. Preparation of filaments

In this work two different starting filaments, which were prepared in different ways, were employed. The starting polymer for filament A was a linear polyethylene Hi-fax 1900 ($\bar{M}_w \approx 4 \times 10^6$ kg kmol^{-1}, $\bar{M}_n \approx 2 \times 10^5$ kg kmol^{-1}). Filament B was produced from a mixture of linear PE Hostalen Gur ($\bar{M}_w \approx 1.5 \times 10^6$ kg mol^{-1}, $\bar{M}_n \approx 2 \times 10^5$ kg kmol^{-1}) and Marlex 6002 ($\bar{M}_w \approx 2 \times 10^5$ kg kmol^{-1}, $\bar{M}_n \approx 2 \times 10^4$ kg kmol^{-1}), in the weight ratio of 95:5. The mixture was originally prepared for reasons outside the framework of this paper.

In both cases, 5 wt% of the starting polymer was dissolved in paraffin oil (containing 0.5 wt% DBPC anti-oxidant) at 150° C, and homogenized for two days at this temperature. Upon cooling, this solution formed a gel, which was cut into pieces that could be fed to the spinning apparatus. Filament A was spun in a Reifenhauser S 013-25 extruder at 170° C. A conical die with an entrance angle of 6° and an exit diameter of 1.8 mm was employed. Spinning and take-up speeds were equal and amounted to 50 cm min^{-1}. For the production of filament B a Göttfert MRD 19 viscometer was utilized. After a homogenization period of 4 h at 169° C, the gel was extruded through a circular die of 1 mm diameter and collected on a take-up bobbin at a distance of 0.5 m from the die exit. The extrusion draw ratio, i.e. the ratio of the take-up speed to the free-extrusion rate (6 cm min^{-1}), was set at 16.4. The paraffin oil was extracted from the filaments by prolonged immersion in hexane at room temperature, which was followed by drying in vacuum at 50° C.

2.2. Drawing experiments

Drawing of short (ca. 1.5 cm) pieces of filament was carried out in a dynamometer [12] under nitrogen at temperatures of 120 and 144° C (filament A), or 108° C (filament B). The temperature variation along the sample was within 1° C. Drawing rates of 3 or 0.12 mm min^{-1} were applied, which corresponds to initial elongation rates of 3.3×10^{-3} and 0.13×10^{-3} sec^{-1}, respectively. Stress–strain curves recorded during drawing showed that no slip of the sample in the dynamometer clamps occurred.

In view of the inhomogeneous nature of the deformation, the draw ratio of a small part of filament chosen for examination in the scanning electron microscope may differ substantially from the overall draw ratio calculated from the distance between the clamps. In order to obtain a better estimate of the relevant draw ratio, ink marks were placed along the sample at a distance of approximately 1.5 mm in the case of filament B. The draw ratio was determined from the initial and final distance between the centres of the marks, as measured by means of a cathetometer.

2.3. Characterization of the morphology

The samples were gold-covered prior to examination in an ISI DS-130 scanning electron microscope (SEM) operated at 20 to 40 kV. For a more quantitative evaluation of the drawing process on a morphological scale, the distribution of interlamellar distances and that of fibril diameters were determined from a large number of measurements on SEM micrographs. For this purpose, 15 × 20 cm^2 photographs presenting a magnification of approximately 18×10^3 or 36×10^3 were examined. The appropriate dimensions were measured by means of a ruler which allowed a subdivision into categories differing by 0.25 mm on the

micrograph. This corresponded to 13.9 and 6.9 nm for interlamellar distance and fibril diameter, respectively. Histograms of the aforesaid quantities were prepared accordingly.

3. Results and discussion

3.1. Deformation of an as-extruded filament

Filament A was obtained by extrusion of a gel of 5 wt% Hi-fax 1900 in paraffin oil at 0.5 m min^{-1}. As shown by Fig. 1, its morphology is characteristic of filaments produced under conditions of free extrusion, i.e. without drawing in the spinning line. Filament A is a very irregular, porous aggregate of polyethylene lamellae, with little overall orientation [11]. In fact, the sample of Fig. 1 was kept taut between the clamps of the dynamometer at 120° C, so as to represent the state corresponding to a draw ratio $\lambda = 1$. The morphology, as observed on SEM micrographs, turned out to be essentially the same as for the untreated sample. There is no sign of any fibrils pointing to the underlying structure of molecular entanglements.

Drawing of filament A in the dynamometer at 120° C was found to proceed inhomogeneously on the macroscopic scale. Overall values of the draw ratio λ were determined which will be only approximate with respect to the sample parts shown in the SEM micrographs. Fig. 2 represents a part of the surface of a filament which was drawn to a ratio of 1.5 at 120° C. Drawing has resulted in the formation of large cavities, which are spanned by fibrils and which are very similar to crazes in glassy polymers [13–16]. Donald and Kramer [17] have pointed out that, in glassy polymers, the fibrillation itself is a direct consequence of molecular entanglements. Further extension results in a diminution of the entities from which the fibrils are drawn, and a concomitant reduction of their lateral size. This is shown in Fig. 3, for a draw ratio of 4. Eventually, this leads to a highly fibrillar morphology with thinly dispersed lumps from which many fibrils originate. The highest draw ratio attained at 120° C amounted to 40. In the range of high draw ratios the changes in the morphology were slight, and Fig. 4 ($\lambda = 15.9$) is a good representative of these structures.

The SEM micrographs show that also on a microscopic scale, the deformation proceeds very

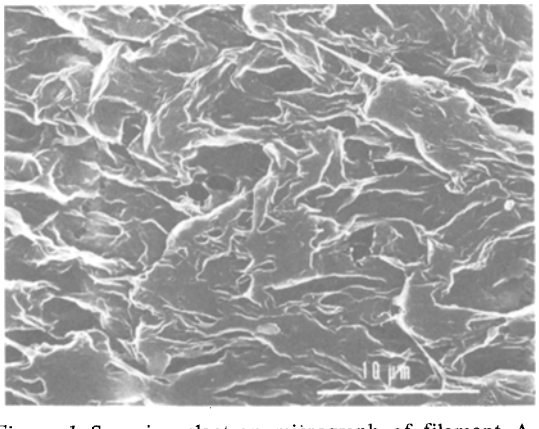

Figure 1 Scanning electron micrograph of filament A, spun from a 5 wt% gel of Hi-fax 1900 in paraffin oil at 170° C. This sample has been kept taut in the dynamometer at 120° C. It shows an irregular, porous, lamellar morphology.

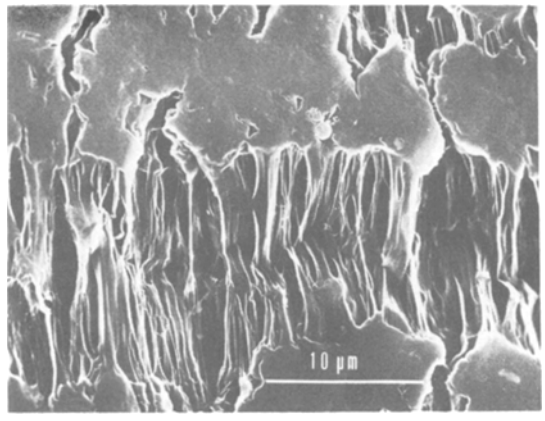

Figure 2 SEM micrograph of filament A drawn in the dynamometer at 120° C to a draw ratio of 1.5. The elongation rate amounted to 3 mm min^{-1}. The fibrillation phenomenon bears a strong resemblance to crazing in glassy polymers.

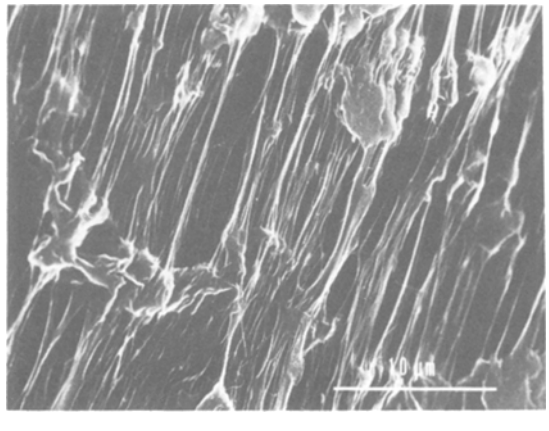

Figure 3 SEM micrograph of filament A drawn to a ratio of 4.0 at 120° C, at a rate of 3 mm min^{-1}. The size of the lumps of lamellae has strongly decreased.

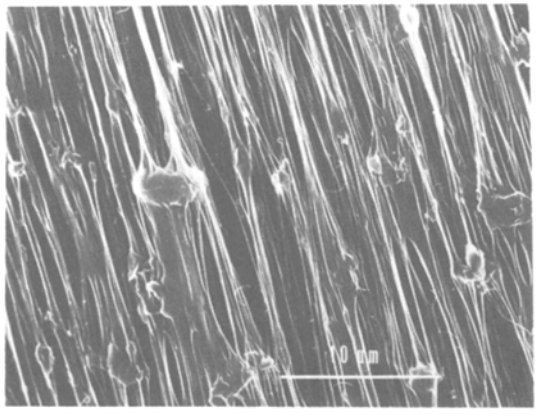

Figure 4 SEM micrograph of filament A drawn to a ratio of 15.9 at 120° C, at a rate of 3 mm min^{-1}. A highly microfibrillar morphology has been formed.

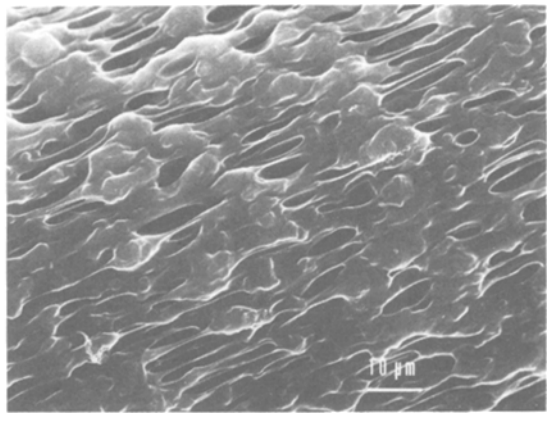

Figure 6 SEM micrograph of filament A drawn to a ratio of 7.5 at 144° C, at a rate of 3 mm min^{-1}. Further drawing has produced more distinct globular entities and longer fibrils in the pores between them.

inhomogeneously. In its initial stages it bears a strong resemblance to crazing phenomena.

In a subsequent series of experiments on the filament A, the drawing temperature was increased to 144° C. This temperature can be considered to be close to the lower bound of the optimum hot-drawing range established for the preparation of ultra-strong polyethylene fibres [18]. Drawing in this range is accompanied by migration and removal of defects and by an increase in crystal continuity [19]. Figs. 5 and 6 show SEM micrographs of filaments drawn to ratios of 2 and 7.5 respectively. (Please note that the magnification is lower than for the previous micrographs.) It is found that the degree of aggregation is much higher than at 120° C. A micron-range porosity is present and has developed further at the higher draw ratio. Apparently, fibrils are pulled out of the globular entities, and in this respect the process is similar to that observed at 120° C. At 144° C, the visible entities are all aggregates, however, and no fibrils or lamellar platelets in the 10 to 100 nm range are observed. SAXS studies have already indicated that at 144° C no porosity on that scale remains, but fibre materials heated or drawn above 140° C have shown a long period of 40 to 45 nm after cooling down [20].

The origin of this period is revealed in Fig. 7, which gives detail of a sample drawn to $\lambda = 5.5$. The surface displays a striation with a period of approximately 40 nm. In Fig. 8 the period

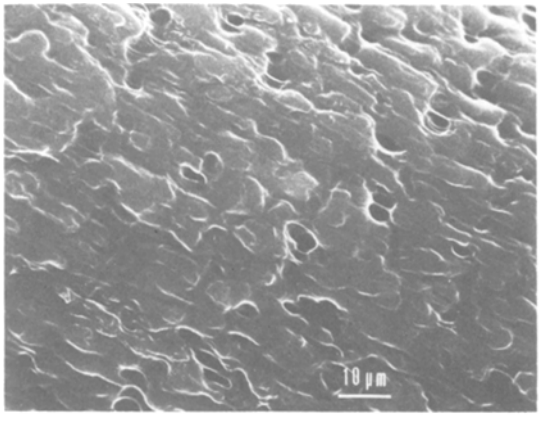

Figure 5 SEM micrograph of filament A drawn to a ratio of 2.0 in the dynamometer at 144° C, at an elongation rate of 3 mm min^{-1}. The morphology shows the presence of globular heterogeneities which, when drawn apart, leave micron-range pores spanned by fibrils.

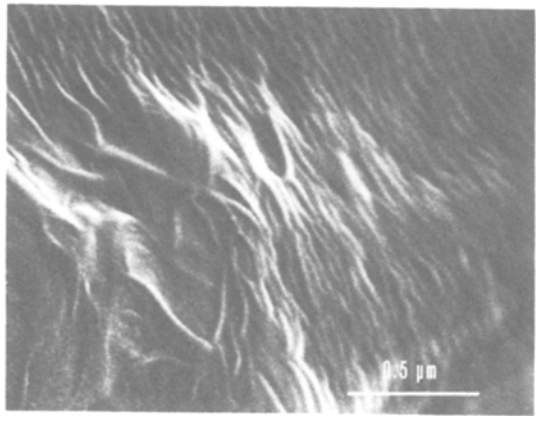

Figure 7 High-resolution SEM micrograph of a sample of filament A drawn to a ratio of 5.5 at 144° C, at a rate of 3 mm min^{-1}. The surface shows a striation, which reflects the lamellar nature of the globular entities in Figs. 5 and 6. The long period amounts to 40 nm.

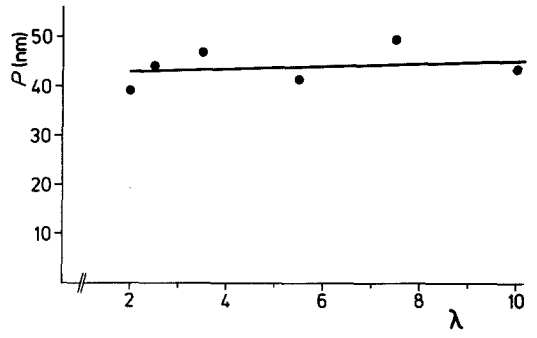

Figue 8 The long period P as a function of the draw ratio λ for samples of filament A drawn at 144° C, at a rate of 3 mm min^{-1}. P has been determined from SEM micrographs.

measured from SEM micrographs for various draw ratios λ is plotted: the long period is independent of the draw ratio, which agrees with the SAXS results. Since SAXS measures bulk properties, the reduction and eventual disappearance of the SAXS peak at high draw ratios was ascribed to a progressive transformation of the semi-crystalline phase in which the 40 nm period resides [20]. This interpretation is easily reconciled with the micrographs shown, which relate the 40 nm period to the globular entities. The globular entities originate from the disordered regions in the cluster-flow units present during gel-spinning [9]. These disordered regions will crystallize in the form of lamellar platelets in the gel filament. When the dried filament is reheated above the melting temperature of the lamellae, the latter will coalesce and the porosity decreases accordingly. Upon hot-drawing, the intrinsic structural heterogeneity of the molten phase causes the elastic liquid to break up into globular entities connected by fibrils of aggregate character. During further drawing, the fibrils grow in length at the cost of the size and amount of the globular entities. The remaining globules, in which a high concentration of entanglements is retained, recrystallize into a dense semi-crystalline phase with a 40 nm long period. A model of this concept is outlined in Fig. 9.

In connection with this, we refer to the work of Rault and Robelin [21], who showed that the long period in polyethylene is uniquely determined by the temperature of the melt before crystallization, for high enough cooling rates. In that case, the occurrence of conformational changes which lead to coil expansion during cooling is limited. Another important factor is the residence time in the melt, which should be much longer than the molecular relaxation time in order that the melt state attains its equilibrium characteristics. These relaxation times were determined from melt-annealing experiments.

For our very high molecular weight polyethylene, the relaxation times are likely to be of the order of hours. During the hot-drawing process, therefore, any conformational changes can be entirely attributed to the flow field generated by the deformation. The initial long period of 40 nm is not determined by the drawing temperature, but it is characteristic of aggregated shish-kebab morphologies and related to the exceptionally large molecular weight between entanglements in the gel filament [22, 23]. The observed invariance of the long period with the draw ratio indicates that the molecular conformation in the globular aggregates is not essentially changed during drawing. This, in turn, suggests that chain extension is a very localized process, in which only a minor fraction of the molecules is involved at a time. The inhomogeneous character of the deformation, as revealed by the micrographs, certainly supports this "micro-necking" model.

Another salient point concerns the length of the crystallites in these hot-drawn gel-spun fibres. X-ray investigations have shown the weight-average crystallite length to increase with increasing draw ratio [23]. In terms of our structural model presented above, this increase with λ indicates that the newly formed fibrils contain longer crystallites than the globules from which these fibrils are drawn. The initial crystallite length amounts to approximately 30 nm and rises to a weight-average value of 70 nm for very high draw ratios. A most conspicuous fact is that the ultimate crystallite length is larger than the SAXS long period of 40 nm. Similar results were obtained by Gibson, Davies and Ward [24] for cold-drawn and hydrostatically extruded polyethylene. This phenomenon is easily accounted for when it is noted that the measured crystallite length is an average over the whole crystalline phase, whereas the SAXS long period pertains only to the globular entities. No SAXS long period (up to 100 nm) was detected in the fully drawn fibres, which indicates that chain backfolding will be very rare in the fibrillar units. SAXS, therefore, suggests a continuous structure of the fibrils. The diffraction coherence of crystals, however, may be limited to 70 nm by crystal torsion, by kink bands or other

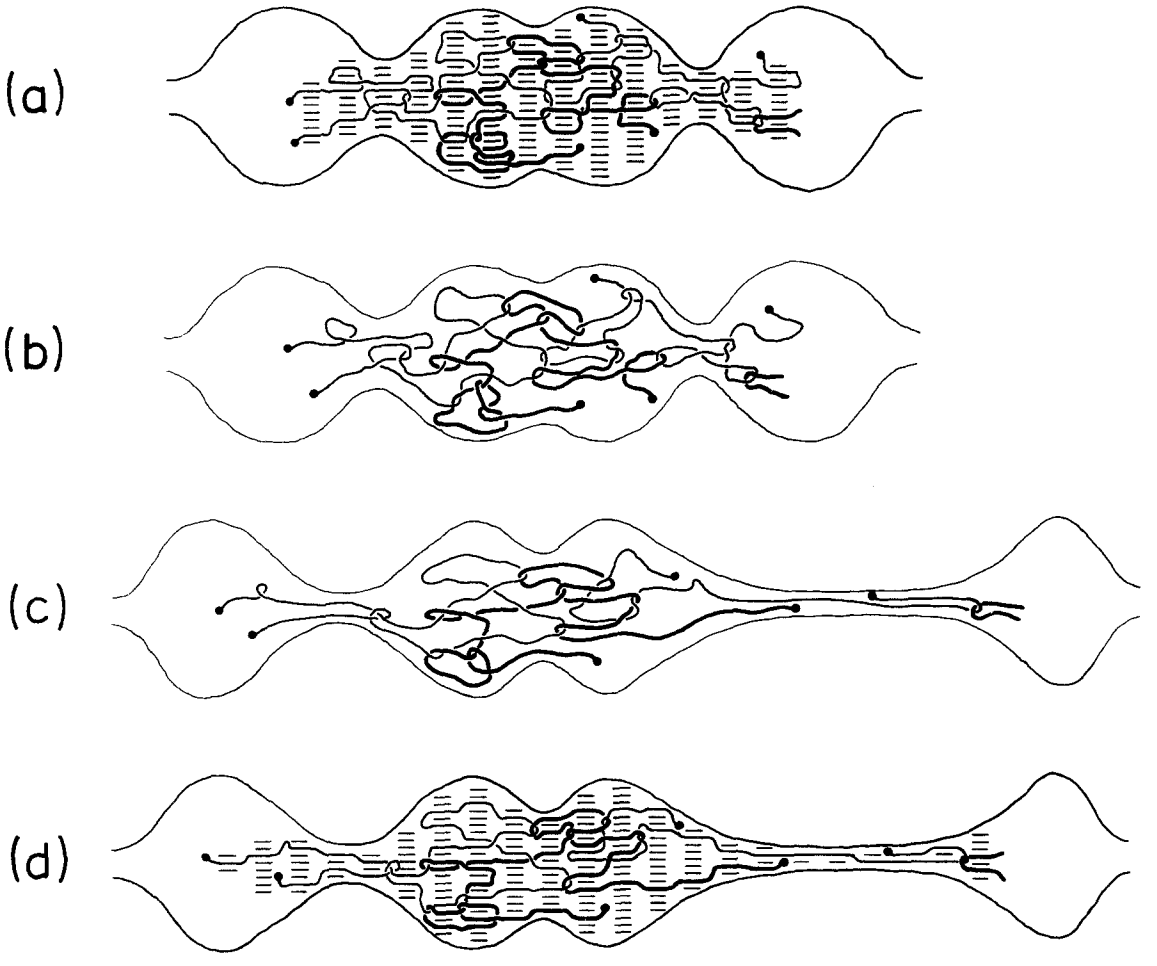

Figure 9 Molecular model for the mechanism of hot-drawing of gel-spun filaments. The emphasis is on the conformation of entangled molecules, of which three are shown. The contours of the model may be identified with the curved boundaries of the morphological entities shown in Figs. 5 and 6, but they are inevitably out of scale and indicated primarily to suggest a certain structural coherence. The initial gel-spun filament is supposed to be lamellar in nature. After a treatment at temperatures above 140° C, the interlamellar porosity is lost and the material recrystallizes in a dense phase with a long period of 40 nm (a). This long period is determined by the chain entanglement topology originating from the gel state. The entanglement network is not essentially affected when it is kept at the drawing temperature for a short period of time (b). Upon drawing, however, certain molecules are extended and some entanglement couplings are released (c). In the regions of higher entanglement density, the molecular conformations are only slightly altered, and these chains recrystallize with the same long period as before (d).

defects. In view of the experimental uncertainties associated with this kind of determination, the value of 70 nm may be an underestimate.

The increase of the crystallite length with draw ratio is well in line with the results of Capaccio and Ward [25, 26], who derived complete length distributions by means of GPC analysis of drawn polyethylene samples subjected to nitric acid etching. The tails of these distributions even extend to crystallite lengths of several hundreds of nm.

3.2. Deformation of an extrusion-drawn filament

The filament B was prepared from a 95:5 mixture of Hostalen Gur and Marlex 6002. A gel, consisting of 5 wt% of this mixture in paraffin oil, was slowly extruded (0.06 m min^{-1}), but drawn to a ratio of 16.4 in the spinning line by the take-up apparatus. This extrusion drawing results in the formation of shish-kebab-type elementary fibrils, as shown in Fig. 10, which is explained by the concept of cluster flow [9].

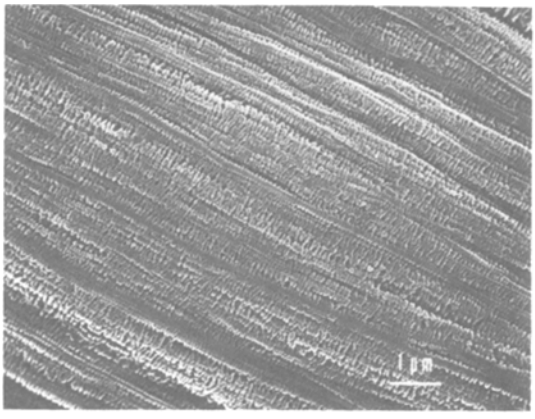

Figure 10 SEM micrograph of filament B, spun from a 5 w% gel of a 95:5 mixture of Hostalen Gur and Marlex 6002 in paraffin oil at 169° C. A morphology of shish-kebab fibrils has been formed as a result of extrusion drawing to a ratio of 16.4 in the spinning line.

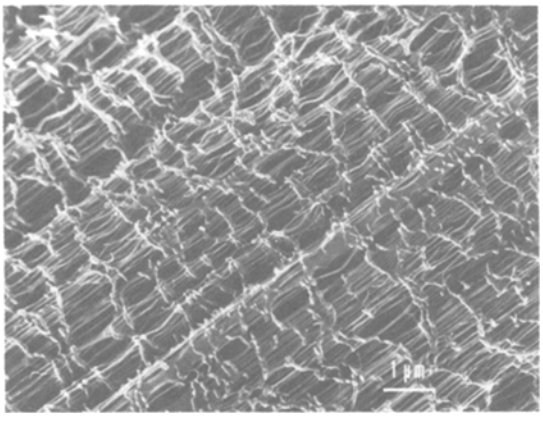

Figure 12 SEM micrograph of filament B drawn to a ratio of 3.0 at 108° C, at a rate of 3 mm min^{-1}. Inhomogeneous deformation has resulted in bunches of lamellae separated by long fibrils.

Pieces of filament were drawn in the dynamometer at 108° C. This temperature allowed reasonable deformations without premature melting of the shish-kebab lamellae. The lower optimum temperature as compared with 120° C for filament A, may be due to the presence of low molecular weight Marlex. Ink marks on the sample have allowed a more reliable determination of the draw ratio of pieces selected for examination in the scanning electron microscope. The micrograph of Fig. 11 shows a sample drawn to $\lambda = 1.35$ at a rate of 3 mm min^{-1}. The interlamellar distances have increased remarkably. For larger values of the draw ratio it is observed that the lamellae remain grouped in bunches, as is demonstrated in Fig. 12 for $\lambda = 3.0$. Within the bunches, the interlamellar distance remains unchanged, whereas much longer interlamellar fibrils are found between the bunches. Since the behaviour of lamellae on adjacent fibrils is rather coherent, the overall picture is (again) reminiscent of crazing: gaps of considerable lateral extent are spanned by smooth fibrils.

On the micrograph of Fig. 13, taken from filament B drawn to $\lambda = 6.9$, individual lamellae are no longer visible. Apparently, the lamellae have melted, which has resulted in the formation of aggregates. It is no longer possible to obtain a reliable value of the average interlamellar distance *P*. These phenomena have been found in samples drawn to $\lambda = 5$ and higher. Since the drawing temperature is only 108° C, this effect must be ascribed to an unusual instability of the crystal

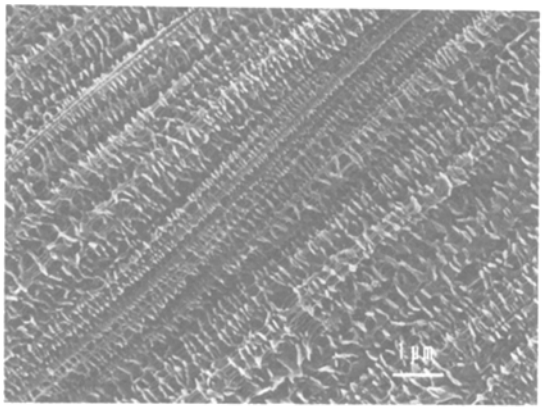

Figure 11 SEM micrograph of filament B drawn to a ratio of 1.35 in the dynamometer at 108° C. The elongation rate amounted to 3 mm min^{-1}. The interlamellar distances are much larger than in Fig. 10.

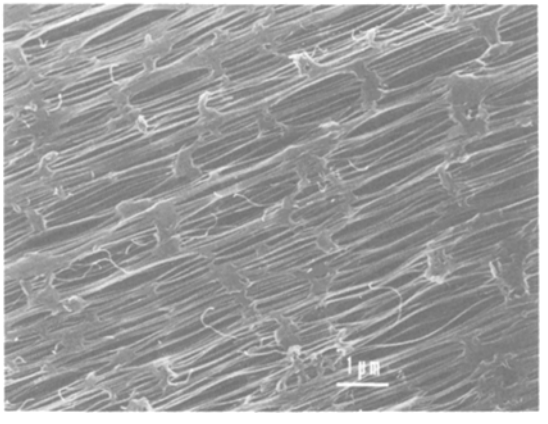

Figure 13 SEM micrograph of filament B drawn to a ratio of 6.9 at 108° C, at a rate of 3 mm min^{-1}. Premature melting of the lamellae has resulted in a more aggregated morphology.

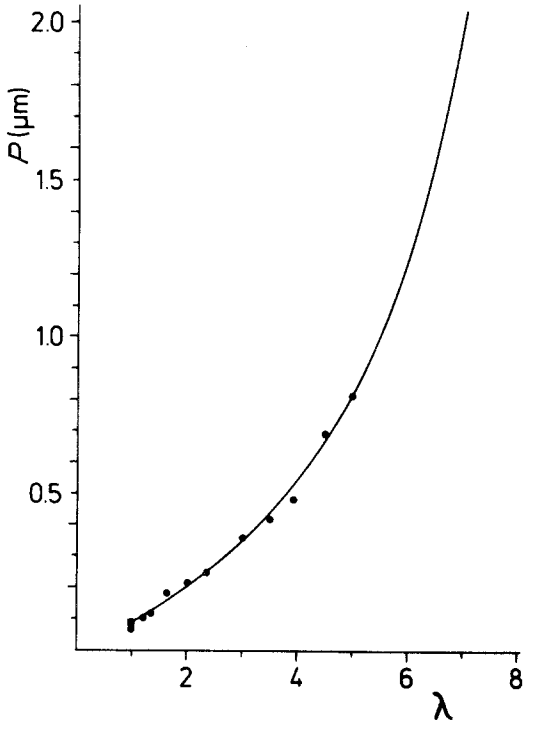

Figure 14 The lamellar period P, as measured from SEM micrographs, as a function of the draw ratio λ for samples of filament B drawn at 108° C, at a rate of 3 mm min^{-1} (•). The solid curve has been calculated from a least-squares fit in which a correction was applied to the lamellar period in the starting material (▪ corrected point). For details see next section.

structure of the lamellae. A possible explanation will be presented in the next section.

The values of P as a function of λ have been plotted in Fig. 14; only those λ-values for which a sufficient number of distinct lamellae could be observed on the micrograph are included. The data points beyond $\lambda = 4$ indicate that P is not linearly proportional to λ, but increases at a higher rate. This suggests that a fraction of the amount of lamellae disappears completely in the course of the extension process. This point will be elaborated in more detail below. It implies, however, a transformation of the lamellae into fibrils, for which a molecular model was proposed in a previous paper [7]. In the model, the lamellae are considered to consist mainly of chain loops. During deformation, these loops are straightened as far as possible, which will inevitably require the transport of some chains through the crystal lattice and the fracture of others. In the final, drawn-out state, some irremovable topological defects such as trapped entanglements remain.

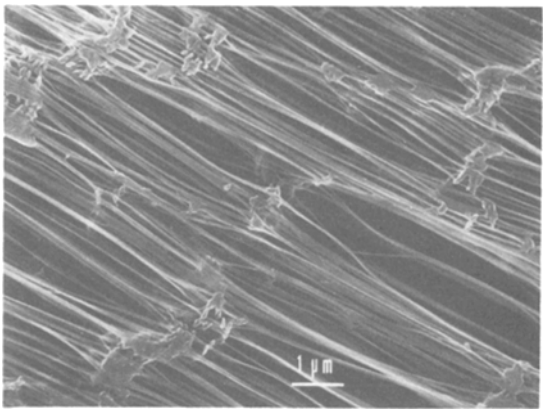

Figure 15 SEM micrograph of filament B drawn to a ratio of 7.9 at 108° C. A very low elongation rate of 0.12 mm min^{-1} was applied and was found to suppress disruption of the lamellae.

Our observations will be discussed in the light of this process.

In an attempt to attain high draw ratios, samples of filament B were drawn at a very low rate of 0.12 mm min^{-1} instead of 3 mm min^{-1}. Fig. 15 shows a sample slowly drawn to $\lambda = 7.9$. At some places the lamellae are found to be less smeared than in Fig. 13, presumably as a result of the lower drawing rate. The same holds for the sample drawn to $\lambda = 8.7$, of which detail is shown at a higher magnification in Fig. 16. A bunch of lamellae is held together by many interlamellar fibrils. At the "outside", just as many fibrils are seen to emanate from the bunch, but they merge into a thick aggregate fibril.

The highest draw ratio attained in the experi-

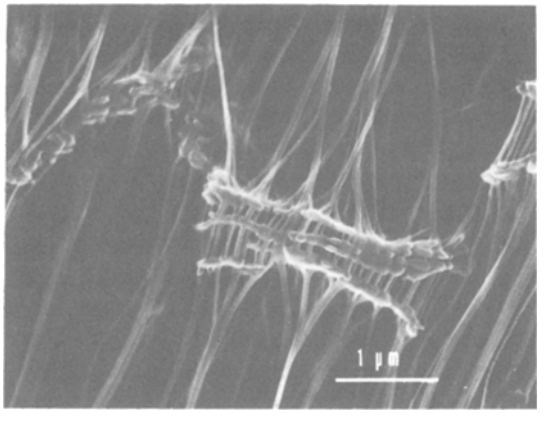

Figure 16 High-resolution SEM micrograph of filament B drawn to a ratio of 8.7 at 108° C, at a rate of 0.12 mm min^{-1}. The many interlamellar fibrils have prevented this bunch of lamellae from being drawn out.

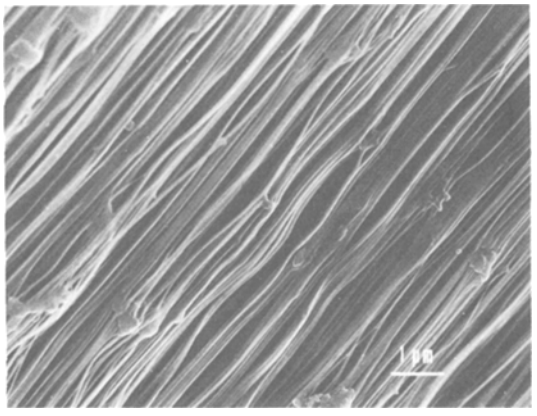

Figure 17 SEM micrograph of filament B drawn to break at 108° C at an elongation rate of 0.12 min min^{-1}. The draw ratio amounted to 27.7. Relatively smooth and slightly aggregated fibrils are found.

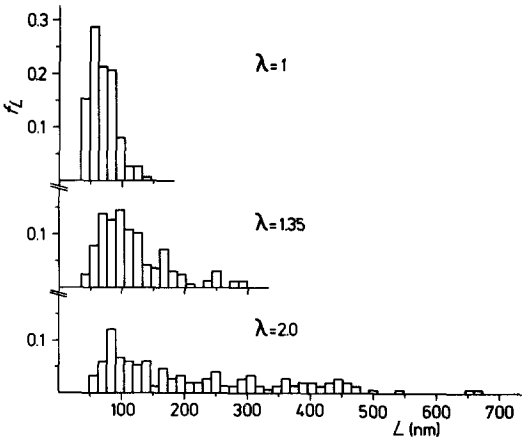

Figure 18 Frequency distributions f_L of interlamellar distances L for three samples of filament B: undrawn and drawn to ratios of 1.35 and 2.0, respectively. Drawing temperature 108° C; elongation rate 3 mm min^{-1}.

ments on filament B amounted to 27.7. The final morphology is free of lamellae as a result of the lamella-fibril transformation (Fig. 17). In the globular irregularities that remain on the fibrils, the molecular topology may be such that incorporation into the fibrils is impossible. Some of these globules may be remnants of fibrils which have ruptured and contracted during drawing.

In the calculation of the average interlamellar distance P, the whole distribution of interlamellar distances was determined for some samples of low draw ratio. Fig. 18 presents three of these distributions. The most important aspect is that the initial distribution ($\lambda = 1$) shows a single peak, whereas for the drawn fibres an additional "tail" of subsidiary maxima appears. This tail rapidly grows out with increasing λ. (No statistical significance is imparted on the details in it, however.) The retention of the main peak reflects our observation that the lamellae remain grouped in bunches. Furthermore we note that the main peaks for $\lambda = 1.35$ and $\lambda = 2.0$ are shifted with respect to the initial peak. At higher draw ratios, the number of lamellae occurring on the micrographs is too small for statistical evaluation beyond averaging.

In addition to the interlamellar distances, the distribution of fibril diameters was determined for several samples. In these measurements, only those fibrils which were clearly individual were considered, aggregates were left out. Some distributions are shown in Fig. 19. In Fig. 20, the average fibril diameter $\bar{d}$ is plotted over a much larger range of λ-values. These graphs show that the average fibril diameter changes little with draw ratio. Since the interlamellar distance P does increase, the constant diameter requires that new fibrillar material is formed. This is the most convincing indication of the lamella-fibril transformation. Moreover, even the shape of the diameter distribution is only moderately altered by drawing. This suggests that the existing interlamellar fibrils are retained during drawing, and that the cross-sectional characteristics of the newly formed fibrils are similar to those of the original ones.

The values of the fibril diameter are less accurate, however, which is due to the presence of a gold layer on the sample, deposited for SEM. According to our estimates, the thickness of this layer will be between 5 and 10 nm, which corresponds to the diameter of the thinnest fibrils that were observed. When this correction is applied to the data in Fig. 20, the average fibril diameter amounts to 15 nm. The apparently lower $\bar{d}$-values for λ around 1 can be explained by the crowding of the lamellae, which effectively shield the fibrils from the gold-beam. In these cases a smaller gold-correction applies.

3.3. A simple, quantitative model for the deformation of shish-kebabs

As a first attempt to account for the data presented above in a quantitative way, we will consider a simple model for the lamella-fibril transformation (Fig. 21). The following assumptions are made:

1. The density of polyethylene in the lamellae is equal to that in the fibrils.

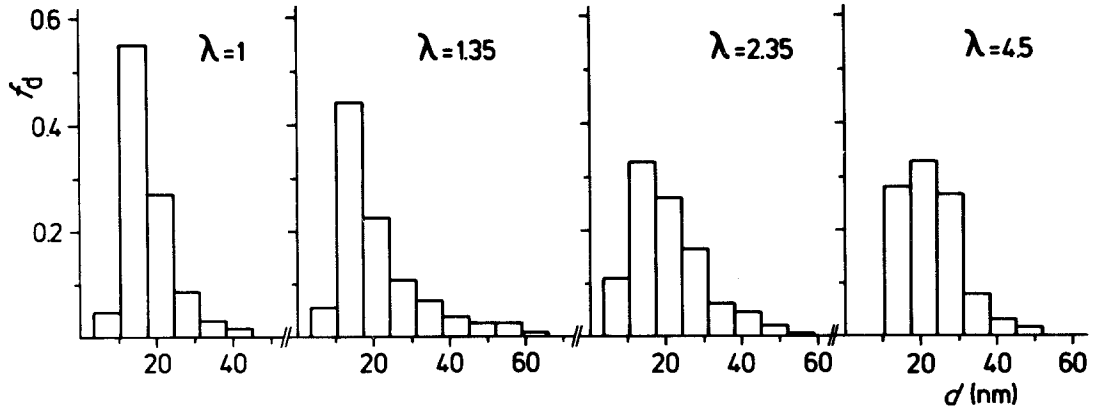

Figure 19 Frequency distributions f_d of fibril diameters d for four samples of filament B: undrawn and drawn to $d = 1.35$, 2.35 and 4.5, respectively. Drawing temperature 108° C; elongation rate 3 mm min^{-1}.

2. When a lamella yields, it is entirely transformed into a fibril segment in a one-step process.

3. Original and newly formed fibril segments are smoothly joined and indistinguishable.

In order to simplify the calculations, the rather heterogeneous morphology of shish-kebabs will be described by single values for the following geometrical parameters:

L: the centre-to-centre distance between adjacent lamellae; it will be simply referred to as the interlamellar distance.

L_0: the interlamellar distance in the undrawn shish-kebab.

t: the thickness of a lamella as measured along the fibril direction.

D: the "diameter" of a lamella, i.e. a dimension such that $\pi D^2/4$ is the cross-sectional area of the lamella in a plane perpendicular to the fibrils. (Since in a real system large lamellae are found which extend over many fibrils, the area must be calculated per traversing fibril.).

d: the diameter of the interlamellar fibrils.

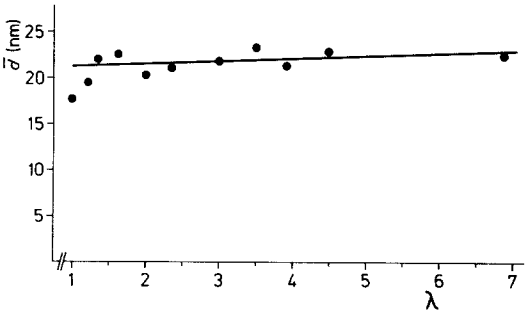

Figure 20 The number-average fibril diameter $\bar{d}$ as a function of the draw ratio λ for samples of filament B drawn at 108° C, at a rate of 3 mm min^{-1}.

Additional parameters of interest are:

a: the length of a fibril segment into which a lamella can be transformed.

F: the length of an original interlamellar fibril + the length of a newly formed segment; $F = (L_0 - t) + a$.

P: the "lamellar period", i.e. the number-average value of the interlamellar (centre-to-centre) distances L of a shish-kebab; for $\lambda = 1, P = L_0$.

The relations given below still hold when number-average values are submitted for the longitudinal (L_0, t, a) and the cross-sectional (D^2, d^2) parameters. Specific correlations are neglected by this approach, however. Since the model implies that the interlamellar distance L in a partly drawn shish-kebab is non-uniform, it must be characterized by a number-average value, namely the lamellar period P.

A constant density implies conservation of volume when a lamella (t, D) is transformed into a fibril segment (a, d):

$$a \times d^2 = t \times D^2 \qquad (1)$$

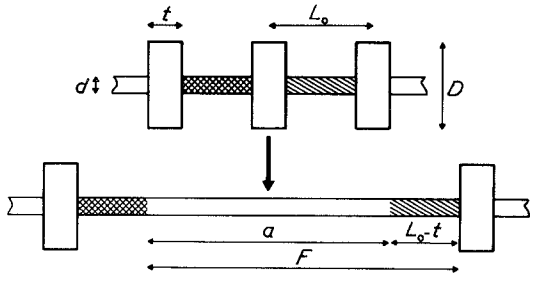

Figure 21 A morphological model for the drawing of shish-kebab fibrils: the transformation of a lamella into a fibril segment. The meaning of the various parameters is discussed in the text.

Suppose that a number fraction ϵ of the lamellae is converted at a certain stage of the drawing process. The elongation factor of an arbitrary length of fibril on which a large number, N, of lamellae were present before drawing, amounts to

$$\lambda = \frac{\text{extended lenth}}{\text{initial length}} = \frac{N(1-\epsilon)L_0 + N\epsilon F}{NL_0} = \frac{L_0 - \epsilon L_0 + \epsilon(L_0 - t + a)}{L_0} = \frac{L_0 + \epsilon(a-t)}{L_0} \quad (2)$$

When combined with Equation 1 this yields

$$\lambda = 1 + \frac{\epsilon t(D^2/d^2 - 1)}{L_0} \quad (3)$$

or

$$\epsilon = \frac{L_0(\lambda - 1)}{t(D^2/d^2 - 1)} \quad (4)$$

The lamellar period of the drawn fibril equals

$$P = \frac{\text{extended length}}{\text{number of lamellae left}} = \frac{N\{(1-\epsilon)L_0 + \epsilon F\}}{N(1-\epsilon)} = \frac{L_0 + \epsilon(a-t)}{1-\epsilon} \quad (5)$$

When this is substituted into Equation 2, the unknown parameters a and t are eliminated:

$$\frac{P}{L_0} = \frac{\lambda}{1-\epsilon} \quad (6)$$

This equation can easily be found by simple arguments, too. The increase of the lamellar period is governed by two factors:

1. the elongation of the shish-kebab fibril, a factor equal to λ;

2. the disappearance of the lamellae; their number is changed by a factor $(1-\epsilon)$ and consequently the period is changed by $1/(1-\epsilon)$. Equation 6 predicts that the lamellar period is not simply proportional to λ but that it increases much faster as soon as a substantial amount of lamellae has been converted. This is the basis for our interpretation of the data in Fig. 14.

When Equation 6 is written as

$$\epsilon = 1 - \lambda L_0/P \quad (7)$$

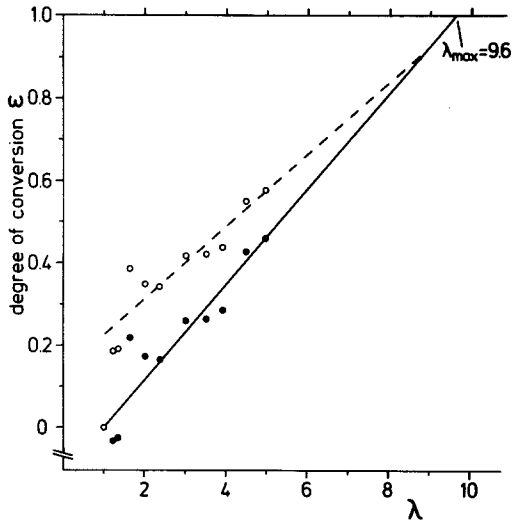

Figure 22 The degree of conversion ϵ (number fraction) of lamellae on the shish-kebab fibrils as a function of the draw ratio λ for samples of filament B drawn at 108° C, at the rate of 3 mm min^{-1}. (○) Data points calculated from Equation 6 with $L_0 = 69.4$ nm; the dashed line is a least-squares fit through all these points except (1, 0). The solid line and the points (●) correspond to a least-squares fit in which L_0 was corrected ($L_{0,c} = 88.3$ nm) so as to fulfil the requirement that the line passes through (1, 0).

it enables us to calculate the degree of conversion ϵ from the known λ-values and the lamellar periods measured from SEM micrographs. The morphological parameters which cannot be accurately determined do not have to be involved at all. In Fig. 22 the calculated ϵ-values have been plotted against λ (open circles). The data scatter considerably. In principle, a relation between the parameters t, d and D could be found by means of this plot and Equation 4. Since t and d may be estimated from the micrographs, the most interesting possibility would be the calculation of D, which is a measure of the lateral extension of the lamellae, in a direction perpendicular to the fibrils. Considerable uncertainties are involved, however, since the deposition of a gold layer on the sample for SEM was found to influence its appearance noticeably. Presumably, the gold layer also produces a deformation of the lamellae, and the estimation of the lamellar thickness t becomes particularly difficult. Moreover, the calculation of D will be very sensitive to inaccuracies in the determination of (λ, P) data for the samples. A calculation of D along these lines is not likely to be very reliable. On the other hand, it would be very difficult to verify D-values with the aid of SEM micrographs, since the lamellae have little

individuality and the relevant number of fibrils which emanates from any one cannot be assessed.

Any D-value calculated from Equation 4 would pertain to the lamellae which have been transformed during drawing up to the ratio under consideration. Our present approach will be based on the simplifying assumption that there is no important variation in the (average) characteristics of the lamellae, whatever the stage at which they are transformed. Small statistical variations will be sufficient to account for the inhomogeneous deformation behaviour from a mechanical point of view. The condition of constant t, d and D for all λ reduces Equation 4 to

$$\epsilon = C(\lambda - 1) \tag{8}$$

The dashed line in Fig. 22 shows that a linear relation holds reasonably well, if the major requirement of passing through (1,0) is released. This points to an erroneous scaling of ϵ and/or λ-values, which may be caused by the experimental procedure. The sample is prestrained in the dynamometer in order to find the initial distance between the ink marks for the calculation of λ. During this prestraining, the interlamellar distance L_0 may increase by straightening of slack fibrils and by elastic deformation, without actual transformation of lamellae. The lamellar distance distributions of Fig. 18 support this explanation: the main peak at approximately 60 nm for the untreated starting sample is shifted to approximately 80 nm for the drawn filaments. Concomitantly, the value of L_0, which was calculated to be 69.4 nm from Fig. 10, must be increased by a prestrain factor.

The corrected initial lamellar period, $L_{0,c}$, and the value of C in Equation 8 were found from a least-squares fit of the data points, in which Δ^2 was minimized with respect to $L_{0,c}$ and C:

$$\Delta = C(\lambda - 1) - (1 - \lambda L_{0,c}/P) \tag{9}$$

The result is represented by the solid line and the filled circles in Fig. 22, and corresponds to

$$L_{0,c} = 88.3\,\text{nm} \tag{10}$$

$$C = 0.116 \tag{11}$$

These values have been used for the calculation of the solid curve drawn in Fig. 14, by means of Equations 6 and 8; a new data point for the starting filament is also indicated.

Knowledge of $L_{0,c}$ and C enables us to calculate two more interesting parameters, the maximum attainable draw ratio and the length F in Fig. 21:

$$\lambda_{max} = 9.6 \qquad \text{(from Equation 8 with } \epsilon = 1) \tag{12}$$

$$F = 850 \text{ nm} \qquad \text{(from Equation 2: } \lambda_{max} = F/L_{0,c}) \tag{13}$$

The calculated value of λ_{max} is much lower than the experimental value of 27.7 for the draw ratio at break (at 0.12 mm min^{-1}). The experimental result can be accounted for by a phenomenon which was not introduced into our model: slip of fibrils past each other. In our view, slip is supposed to set in at a later stage, when a considerable fraction of the lamellae has been converted. At that stage, the matrix of lamellae has become too thin to withstand the shearing forces between fibrils, and the lamellae will be disrupted. The lamellae themselves may have been weakened beforehand by the removal of some molecules from the folded-chain lattice, which may explain the onset of melting as observed in Fig. 13.

The value of F, or rather $F + L_{0,c}$ which is approximately 940 nm, should be reflected in the lamellar distance distributions of the drawn samples (Fig. 18). It is found, however, that interlamellar distances of this size are first encountered for draw ratios of 3 or higher (cf. Fig. 12). They are not present in the fibres for which distributions are given in Fig. 18. These plots, on the other hand, show that a whole range of intermediate distances exists. As a probable explanation, we note that such a spread of interlamellar distances will result when lamellae are only partly transformed into fibrils. Partial transformation is very likely to prevail when drawing is terminated at a low draw ratio. Some aspects of partial transformation will be shortly discussed in the next section.

It should be emphasized that the estimates λ_{max} and F are independent of our knowledge of the morphological parameters d, t and D. The values of C and $L_{0,c}$, moreover, imply a relation between these morphological parameters, and by means of $C = L_{0,c}/\{t(D^2/d^2 - 1)\}$ and $d^2 = 300\,\text{nm}^2$ one finds

1. $D = (\overline{D^2})^{1/2} = 68$ nm for $t = 52$ nm;
2. $D = 73$ nm for $t = 45$ nm;
3. $D = 103$ nm for $t = 22$ nm.

These results correspond to gold-corrections of 0, 7 and 30 nm, respectively, for the lamellar thickness. They seem to be reasonable values for the

"diameter" of the lamellae when considered on a one-fibril-per-lamella basis.

3.4. Some considerations on an improvement of the model

In our simple model of Fig. 21, the possibility of partial transformation was excluded. The inaccuracies in the numerical data derived from SEM micrographs do not justify calculations with a more detailed model. A particular problem arises with regard to the lamellar period P. This quantity bears no information concerning the degree of transformation of individual lamellae, since it is based on a visual evaluation of the SEM micrographs in which all lamellae which are not yet completely transformed are taken into account. In view of the heterogeneous nature of the shish-kebabs in gel-spun filaments, a more detailed evaluation is not feasible.

With respect to a model in which the partial transformation of lamellae is considered, the following remarks can be made. It is found that Equations 2, 3 and 4 presented above still hold in such a model, if ϵ is interpreted as the average degree of transformation over the initial amount of lamellae. In the more general case of variations in the dimensions of the lamellae, ϵ should be replaced by the volume fraction of lamellar phase which has been transformed. In such a more realistic model, possible correlations which have been neglected until now could be taken into account. The preferential transformation of small lamellae, for instance, may in itself produce the spread of interlamellar distances in samples of low draw ratio. As a consequence of the reduced information content of the lamellar period parameter P, the meaning of ϵ in Equation 6 differs from that in Equation 4, and the degree of conversion can no longer be calculated from (λ, P) data for each sample. It is expected that this problem will be less severe at higher draw ratios, when most of the lamellae have been entirely transformed.

3.5. Relation between morphology and flow properties of gel-spun filaments

In recent papers from our laboratory, the preparation of ultra-high strength polyethylene fibres by gel-spinning/hot-drawing has extensively been described [9, 11]. The optimum temperature range for hot-drawing was demonstrated to be 143 to 150° C. In the first investigation into the underlying mechanism, Smook and Pennings [18] have presented data on the elongational viscosity η of gel-spun filaments during hot-drawing, in a range of temperatures between 110 and 148° C and draw ratios between 7 and 36. Some important findings will be summarized here.

1. At temperatures below 130° C the deformation mode was controlled by the considerable porosity of the fibre. It was found necessary to predraw the fibres to a ratio of approximately 5, since the inhomogeneous nature of the deformation would prevent a meaningful determination of η at lower draw ratios;

2. A change in drawing behaviour, viz. an increase of η was observed between $\lambda = 5$ and $\lambda = 10$. This was considered to be a transition region, with the structure becoming truly fibrillar around $\lambda = 8$;

3. From the η-values measured between 110 and 133° C an activation energy of approximately 50 kJ mol^{-1} was derived for drawing above $\lambda = 10$. At these temperatures, therefore, drawing would merely involve slip of fibrils past each other;

4. Above 143° C the activation energy for drawing was found to be higher than 300 kJ mol^{-1}, which suggested a considerable transport of chains through extended-chain blocks, possibly in the hexagonal phase [27, 28].

The agreement with the observations presented in this work is very good, despite the fact that a different starting sample, though of shish-kebab type, was used by Smook and Pennings. It is easily understood that the inhomogeneous microdeformation of a shish-kebab type morphology at low draw ratios, will influence macroscopic flow properties. Pertinently, the transition region between $\lambda = 5$ and $\lambda = 10$ can be identified with the range in which destruction of the lamellae occurs as a result of shearing forces between neighbouring fibrils. The achievement of a truly fibrillar structure at a λ-value beteen 8 and 10 coincides very well with our calculated λ_{max} of 9.6.

A completely different mechanism at 144° C, as previously suggested [18], is clearly demonstrated in Figs. 5 and 6, although a more or less isotropic filament was used in our case. The steady creation of fibrils of such diverse appearance points to mobility on the molecular level and no longer any individuality of lamellae or elementary fibrils. The progressive elongation of the flow units in the Marrucci–Harmans model [29], as applied by Smook and Pennings, can be easily reconciled with this behaviour.

4. Conclusions

The morphological examination of gel-spun polyethylene filaments subjected to a controlled deformation process, has demonstrated the similarity between drawing of polyethylene and crazing phenomena in glassy polymers. The coherent formation of (micro) fibrils indicates the essential role of molecular entanglements in both these processes.

Both at low ($<120^\circ$ C) and high ($>140^\circ$ C) temperatures, the extension process in polyethylene filaments is very inhomogeneous, with many "micronecking" sites distributed throughout the material. Above 140° C a higher degree of aggregation is found, and elementary fibrils have lost their individuality and have merged into fibrils. The lamellae have coalesced into droplet-like aggregates, which recrystallize with a 40 nm long period. The value of this long period does not depend on the hot-draw ratio, which implies that the entanglement topology in the droplets is retained. Through micronecking zones, the material in the droplet is converted into fibrils, which contain crystallites with a length of at least 70 nm. The absence of a SAXS long period emphasizes the continuous character of the crystal structure in these fibrils.

The deformation of individual elementary fibrils has been found to be readily observable in the drawing of pronounced shish-kebab morphologies at 108° C. The transformation of lamellae into fibrils is the primary deformation mode. A maximum draw ratio of 9.6 is predicted from measurements of morphological parameters and the application of a most simple model. Since a much higher draw ratio can be attained experimentally, slip of fibrils past each other must occur in a second stage. This is reflected in shearing and low-temperature melting of the lamellae for draw ratios larger than 5. The occurrence of slip implies that the elementary fibrils have a finite length, as suggested by Peterlin [1–3], or that weak spots are present at which fracture of the (micro) fibrils takes place.

Our conclusions agree very well with those from a previous study of the elongational viscosity of polyethylene filaments during drawing at various temperatures. The deformation of ultra-high molecular weight polyethylene, therefore, can be best described as a flow process. At any stage, the molecular conformations are determined by the flow pattern which satisfies the topological constraints imposed by the entanglements, and so is the morphology after crystallization. The role of the temperature is merely to control the resistance of the morphological units against deformation.

Acknowledgement

The authors would like to thank B. A. Klazema for his electron microscopic work, and Ir. J. Smook for his help in the preparation of fibres.

References

1. A. PETERLIN, *J. Mater. Sci.* **6** (1971) 490.
2. *Idem, Colloid Polym. Sci.* **253** (1975) 809.
3. *Idem,* in "Ultra-High Modulus Polymers", edited by A. Ciferri and I. M. Ward (Applied Science Publishers, London, 1979) Chap. 10.
4. J. PETERMANN, W. K. LUGE and H. G. LEITER, *J. Polym. Sci., Polym. Phys. Ed.* **17** (1979) 1043.
5. P. M. TARIN and E. L. THOMAS, *Polym. Eng. Sci.* **19** (1979) 1017.
6. T. JUSKA and I. R. HARRISON, *ibid.* **22** (1982) 766.
7. P. F. VAN HUTTEN, C. E. KONING and A. J. PENNINGS, *Makromol. Chem., Rapid Commun.* **4** (1983) 605.
8. *Idem, Colloid Polym. Sci,* **262** (1984) 521.
9. J. SMOOK and A. J. PENNINGS, *J. Mater. Sci.* **19** (1984) 31.
10. B. KALB and A. J. PENNINGS, *Polym. Bull.* **1** (1979) 871.
11. J. SMOOK, M. FLINTERMAN and A. J. PENNINGS, *ibid.*, **2** (1980) 775.
12. A. POSTHUMA DE BOER and A. J. PENNINGS, *Macromolecules* **10** (1977) 981.
13. R. P. KAMBOUR and R. R. RUSSELL, *Polymer* **12** (1971) 237.
14. P. BEAHAN, M. BEVIS and D. HULL, *J. Mater. Sci.* **8** (1973) 162.
15. R. P. KAMBOUR, *Macromol. Rev.* **7** (1973) 1.
16. S. WELLINGHOFF and E. BAER, *J. Macromol. Sci. Phys.* **B11** (1975) 367.
17. A. M. DONALD and E. J. KRAMER, *J. Polym. Sci., Polym. Phys. Ed.* **20** (1982) 899.
18. J. SMOOK and A. J. PENNINGS, *J. Appl. Polym. Sci.* **27** (1982) 2209.
19. E. S. CLARK and L. S. SCOTT, *Polym. Eng. Sci.* **14** (1974) 682.
20. P. F. VAN HUTTEN, C. E. KONING, J. SMOOK and A. J. PENNINGS, *Polym. Commun.* **24** (1983) 237.
21. J. RAULT and E. ROBELIN, *Poly. Bull.* **2** (1980) 373.
22. J. DE BOER and A. J. PENNINGS, *ibid.* **7** (1982) 309.
23. J. SMOOK and A. J. PENNINGS, *Colloid Polym. Sci.* **262** (1984) 712.
24. A. G. GIBSON, G. R. DAVIES and I. M. WARD, *Polymer* **19** (1978) 683.
25. G. CAPACCIO and I. M. WARD, *J. Polym. Sci., Polym. Phys. Ed.* **20** (1982) 1107.

26. G. CAPACCIO, *Pure Appl. Chem.* **55** (1983) 869.
27. A. J. PENNINGS and A. ZWIJNENBURG, *J. Polym. Sci., Polym. Phys. Ed.* **17** (1979) 1011.
28. J. C. M. TORFS, "Ultra-Strong Polyethylene Fibers Produced by Crystallization from Flowing Solutions", PhD thesis, Groningen (1983) Chap. 9.
29. G. MARRUCCI and J. J. HERMANS, *Macromolecules* **13** (1980) 380.

Received 18 May
and accepted 4 June 1984